Chemical Engineering Journal 510 (2025) 161636

Contents lists available at ScienceDirect

Chemical Engineering Journal

journal homepage: www.elsevier.com/locate/cej

Demonstration of hydrogen production from food industry wastewaters by solar photoreforming: From the laboratory to outdoors operation in panel reactors

Laura Carolina Valencia-Valero, Kevin A. Simbaña, Jonas E. Eleraky, Monika Hapońska, Alberto Puga *

Departmento of Chemical Engineering, Universitat Rovira i Virgili, Av. Països Catalans, 43007 Tarragona, Spain

ARTICLE INFO

Keywords:
Wastewater treatment
Hydrogen
Photocatalysis
Solar reactors
Solar chemistry
Decontamination

ABSTRACT

The concept of hydrogen production by the photocatalytic reforming (photoreforming) of wastewaters is herein proven for food industry effluents, both in classic batch laboratory cells, and in panel reactors operated under natural sunlight. Initial screening and photocatalyst optimisation, performed employing glucose as a representative model oxygenated contaminant, guided the selection of the most appropriate metal/titania materials for the process. Different metals were compared as co-catalysts in M/TiO_2 (*M*: Cu, Ag, Au or Pt). Enhanced hydrogen production was achieved for platinum as the co-catalyst, regardless of the deposition method used. A hydrothermally synthesised nanosized titania with a partly oxidised carbonaceous coating was compared to commercial anatase and the benchmark P25 anatase–rutile nanocomposite, proving advantageous performance for the former in basic media ($>$ 4.5 mmol(H_2) g_{cat}^{-1} h^{-1}, $c_{glucose}$ = 5 % *w/v*, pH = 12, simulated sunlight). Similarly, the same material outperformed the P25 counterpart for real juice production wastewaters having high pH values. Finally, photoreforming of juice production wastewaters was demonstrated in a novel prototype panel reactor under outdoors solar irradiation over the course of two weeks. Regarding wastewater treatment, pH decreased significantly from *ca.* 11 to $<$ 6 and conductivity also decreased from 2.4 to 1.9 mS cm^{-1}. Organic matter breakdown was confirmed by long-term decrease of chemical oxygen demand and by disintegration of solids. As a final proof of effectiveness of the solar photocatalytic process, daily gas production volumes observed remarkably paralleled sunlight irradiance.

1. Introduction

The management of wastewaters from various industries represents a significant environmental and economic challenge due to their significant contaminant load and large volumes, namely ≈ 400 km^3/y [1,2]. Beyond common and widespread effective wastewater treatment technologies, mostly based on physicochemical and aerobic biological processes, several energy-recovery options are on occasions adopted. The most common of such valorisation technologies entails the sedimentation and decanting of sludges and their ulterior anaerobic digestion, resulting in the generation of biogas [1,3]. Additionally, technologies for multi-fuel generation systems have been developed, enabling process optimisation and reducing environmental impact [4]. Nevertheless, the development of alternative efficient treatment and valorisation of aqueous effluent contaminants, mostly organic in nature, are desirable for reducing their environmental footprint and recovering value-added products [1]. In this context, hydrogen production from wastewater is emerging as a promising strategy [5].

Compared to conventional hydrogen production methods that rely on fossil fuels, such as steam methane reforming and coal gasification, and pure water electrolysis for green hydrogen production [6], waste-to-hydrogen processes are gaining attention as novel sustainable pathways [7,8]. Currently, various research efforts are focused on the use of biomass, as in the case of biorefineries, which, through biological processes such as fermentation, have the capability to produce hydrogen, bioethanol, and biomethane. However, although these processes represent a form of valorisation, they come with certain limitations, such as high energy consumption for production, the management of generated solid waste, and the need for pretreatment of organic matter [9]. On the other hand, using wastewater as a hydrogen source offers dual benefits:

* Corresponding author.
E-mail address: alberto.puga@urv.cat (A. Puga).

https://doi.org/10.1016/j.cej.2025.161636
Received 10 January 2025; Received in revised form 7 March 2025; Accepted 14 March 2025
Available online 15 March 2025

waste minimisation and renewable energy generation. This approach not only provides a means for cleaner effluent treatment but also enables the recovery of energy in the form of hydrogen, making it a highly attractive solution for industries with high wastewater production, such as the food and beverage sector [5]. Unlike thermal processes [10,11], alternative methods like photoreforming, which involves the harnessing of photonic energy by semiconductor photocatalysts, enable hydrogen production at near-ambient conditions and under sunlight irradiation [12–14]. Hence, photoreforming enabled by solar radiation may significantly reduce energy input requirements for the process and enhance its sustainability.

The use of TiO_2-based photocatalysts has been extensively studied for photoreforming due to their chemical stability, low cost, and strong oxidative properties [15,16]. These materials can facilitate the degradation of various organic compounds present in wastewater while generating hydrogen. Nevertheless, the efficiency of TiO_2-based systems is limited due to both rapid recombination of photogenerated electron-hole pairs and predominant absorption in the ultraviolet spectrum, which comprises only a small fraction of solar radiation [17]. To enhance their performance, noble or coinage metals such as platinum, silver, gold or copper are often used as co-catalysts. These metals act as electron sinks, thus reducing charge recombination, and facilitate the hydrogen evolution reaction [18–21].

Several reviews have summarised the advancements in photoreforming, highlighting the importance of catalyst design, reaction conditions, and system configurations in optimizing hydrogen production [22,23]. Additionally, various studies have emphasized the influence of ionic species in the medium, pH, and organic matter concentration on degradation processes. It is essential to take these factors into account to ensure the efficiency of the process in its dual function [24]. Light-promoted waste valorisation through photoreforming and similar techniques is a promising approach for maximizing the value of organic waste streams [25]. Previous studies on photoreforming have demonstrated its versatility in treating various organic substrates, from simple alcohols to complex biomass derivatives or wastewaters. Additionally, advancements in the design of photocatalysts for the selective oxidation of biomass derivatives further underscore the efficacy of photoreforming in converting organic waste into valuable hydrogen [26]. The photoreforming of wastewaters has proven efficient for the dual purpose of both decontamination and hydrogen production, despite scarce literature reports. Seminal investigations by Malato and co-workers indicated both challenges and opportunities for hydrogen production from urban wastewater in pilot-scale solar reactors [27–29]. Industrial effluents containing oxygenated contaminants such as sugars have also been the focus of research efforts on photoreforming [28,30–32]. These findings illustrate the potential of photoreforming for converting diverse wastewater streams into hydrogen.

This work builds on these concepts, focusing on the optimisation of TiO_2-based photocatalysts for the simultaneous production of hydrogen and degradation of organic matter in wastewaters from the food industry. Laboratory-scale experiments under simulated sunlight served to identify favourable conditions to significantly enhance the photocatalytic process. Subsequently, selected experiments were performed on a pre-pilot scale in photocatalytic panels under natural sunlight, showing sustained hydrogen production from real wastewaters and simultaneous degradation of saccharides and other oxygenates. The upscaling transition from laboratory to solar plant operation presented herein demonstrates that solar photocatalysis is a sustainable solution for wastewater treatment and clean energy recovery in real conditions.

2. Experimental section

2.1. Synthesis of photocatalysts

Full details about the reagents and additional chemicals used during synthesis and other experimental procedures are detailed in the Supplementary Material. A description of the synthetic procedures is briefly summarised herein for the sake of conciseness. Three types of nanosized titania were employed, namely:

(i) TiO_2(SA): Anatase, synthesised hydrothermally from titanium isopropoxide in anhydrous acetone (200 °C, 12 h), and subsequently calcined (static air, 200 °C, 2 h) [33].
(ii) TiO_2(CA): Commercial anatase nanopowder.
(iii) TiO_2(P25): Commercial anatase–rutile nanocomposite produced by flame pyrolysis.

Metal co-catalysts were loaded on the surface of titania by a selection of methods to yield a range of M/TiO_2 photocatalysts (*M*: metal; 1 % metal/titania mass ratio), as detailed below.

(i) $^{DP}M/TiO_2$(P25) (*M*: Ag, Cu, Au or Pt), prepared by a deposition–precipitation method on TiO_2(P25) in slightly basic media was adopted, followed by thermal reduction (H_2, 300 °C, 3 °C min^{-1}, 5 h) to perform a metal screening study [30].
(ii) $^{H}Pt/TiO_2$(P25), produced by classical platinum impregnation on TiO_2(P25) followed by calcination (static air, 400 °C, 2 h) procedure, and finally thermal reduction (H_2, 300 °C, 3 °C min^{-1}, 5 h) [34].
(iii) $^{CR}Pt/TiO_2$(P25), prepared by chemical reduction in refluxing alkaline methanol [35,36].
(iv) $^{P}Pt/TiO_2$(P25), $^{P}Pt/TiO_2$(CA), $^{P}Pt/TiO_2$(SA), synthesised by the photodeposition procedure under UV irradiation (365 nm) on different titania supports.

2.2. Photocatalyst characterisation

Full characterisation instruments and procedures are detailed in the Supplementary Material. Crystalline phases were identified by X-ray diffraction (XRD). Morphology and elemental composition were studied by scanning electron microscopy (SEM) coupled with energy dispersive X-ray spectroscopy (EDX). Sizes of metal co-catalyst particles were examined by means of transmission electron microscopy (TEM) or high-resolution transmission electron microscopy coupled to energy dispersive x-ray spectroscopy (HRTEM-EDX). Optical characterisation of the materials was conducted by UV–Vis-NIR diffuse reflectance spectroscopy (DRS). Thermogravimetric analysis (TGA) was carried out under air atmosphere. Surface properties were examined by means of attenuated total reflectance Fourier transform infrared spectroscopy (ATR-FTIR).

2.3. Wastewater analyses

Four wastewater samples (JWW1, JWW2, JWW3, JWW4) derived from the manufacturing of purees, smoothies and juices in pouch, bottle and cup formats, made from fresh food ingredients, chiefly fruit, were generously sourced by Delafruit S.L.U. (La Selva del Camp, Tarragona, Spain). They were characterized by determining physicochemical properties, namely pH, conductivity, and chemical oxygen demand (COD), as listed in Table S1. Furthermore, their chemical composition regarding specific components such as saccharides and organic acids (Table S2), and their evolution during solar photocatalysis, was studied by high-performance liquid chromatography (HPLC). The wastewater samples have broadly different properties and compositions and are difficult to categorise. As a parameter which stands out, pH is almost neutral for JWW1 and noticeably basic for the other three effluents, especially for JWW3 and JWW4 (pH > 12, Table S1). Saccharide contents is particularly high for JWW2 and JWW4, which contain high amounts of sucrose and glucose (1142 and 2295 mg L^{-1}, respectively, Table S2).

2.4. Laboratory-scale photocatalytic activity screening

Batch laboratory-scale photoreforming experiments were performed using photocatalyst suspensions (25 mg, 25 mL) in aqueous glucose (5 % w/v) or wastewater samples in a gas-tight quartz reactor (see Fig. S1) under N_2 atmosphere and simulated sunlight (Xe lamp, AM1.5G, 1000 mW cm^{-1}). Gas samples (2 mL) were analysed by gas chromatography (GC).

2.5. Outdoors photoreforming of wastewaters in a photocatalytic panel reactor

Outdoors photoreforming experiments under natural sunlight were performed in a flat panel reactor developed in our laboratories, as recently described in a patent application [37] (Fig. 1; see extended description in the Supplementary Material and additional schematic illustrations in Fig. S3). The photocatalyst was immobilised by drop-casting on flat surface of the panel basin ($^{H}Pt/TiO_2$(P25), 0.30 g, irradiation area: 0.033 m^2). The panel reactor was closed with a top borosilicate glass window and sealed with polyurethane gaskets.

The panel reactor operates in recirculation mode within a closed circuit, whereby the wastewater flows over the photocatalyst bed, which is immobilised on the panel basin surface and exposed to sunlight; therefore, the operation mode is similar to fixed-bed catalyst configurations. The panel ports are connected via tubes to the recirculation circuit, which includes a wastewater reservoir tank receiving the liquid from the panel and equipped with a liquid outlet port and a gas outlet port connected to a gas accumulation tank. The liquid from the reservoir is flowed by a peristaltic recirculation pump back into the panel reactor. Gas and liquid sampling units are inserted in the gas accumulation tank and upstream the panel inlet, respectively.

Solar photoreforming experiments were performed outdoors under natural sunlight, orienting the panel South at a 30° tilt angle to maximise sunlight incidence during central hours of the day (Fig. S4). A sample of JWW2 (1.5 L) was recirculated continuously (3 L h^{-1}) after purging with Ar, and the system kept under solar irradiation over a period of two weeks during July 2023. Daytime temperatures during solar irradiation ranged from 25 to 30 °C, whereas maximum direct solar irradiances varied significantly, ranging from 121 to 1104 W m^{-2}. Liquid wastewater and gas samples were taken for analysis. Cumulative produced gas volumes and direct solar irradiances were measured daily.

3. Results and discussion

3.1. Photocatalyst characterisation

3.1.1. Titania characterisation

All photocatalysts prepared and used in this work are based on titania as the light-responsive semiconductor material, also serving as the support for metal co-catalysts. Three titania support materials of different crystal phase composition have been studied, *i.e.* hydrothermally synthesized anatase, commercial anatase and benchmark anatase–rutile nanocomposite mixture, *i.e.* TiO_2(SA), TiO_2(CA) and TiO_2(P25), respectively. As observed by TEM measurements, TiO_2 particle sizes increased in the order SA < CA < P25 (Table S3), whereas XRD confirmed the presence of the expected anatase and/or rutile phases (Fig. S5). As observed by SEM, TiO_2(SA) consisted of 0.5–2 μm microspheres composed of small primary nanoparticles (< 10 nm), whereas elemental analysis by HRTEM-EDX revealed well-dispersed presence of carbon (Fig. S6c), most likely as carbonaceous coatings formed due to self-aldol condensation of acetone and subsequent pyrolysis [38]. Further analysis by FTIR of TiO_2 (SA) indicated additional signals (1560, 1440 cm^{-1}; Fig. S6d) attributable to carboxylate groups in the carbon layer [39–41,55] which could influence optical and catalytic properties, as discussed below. The amount of such carbonaceous component was estimated by TGA as 3–4 % by mass (Fig. S6f).

3.1.2. Characterisation of deposited metal co-catalysts

Metal loading had little impact on titania phases in the resulting *M*/TiO_2, as expected (Fig. S5). Due to the small nanoparticle sizes of metal co-catalyst species (see measurements by TEM in Table S4 and micrograph examples for $^{DP}M/TiO_2$ in Fig. S7), no additional peaks were observed by XRD [30,42]. The effect of deposition method on metal particle sizes was studied for platinum on P25, revealing that Pt sizes decreased in the following order: $^{CR}Pt/TiO_2$ > $^{P}Pt/TiO_2$ > $^{H}Pt/TiO_2$ > $^{DP}Pt/TiO_2$. Based on previous reports indicating enhanced photocatalytic hydrogen production for 1–2 nm Pt nanoparticles [43,44], $^{H}Pt/TiO_2$ was employed as a reference photocatalyst for the final validation of the panel reactor (see below). The effect of the TiO_2 support on the size of Pt particles was investigated for the photodeposition method, showing that Pt particle sizes increase in the order $^{P}Pt/TiO_2$(SA) < $^{P}Pt/TiO_2$(CA) < $^{P}Pt/TiO_2$(P25); remarkably small platinum nanoparticles (< 2 nm) were loaded on pure phase anatase titania supports (Fig. S8, Table S4). Given the particle size control achieved and the amenable procedure, photodeposition was chosen as the loading method for further photocatalyst screening.

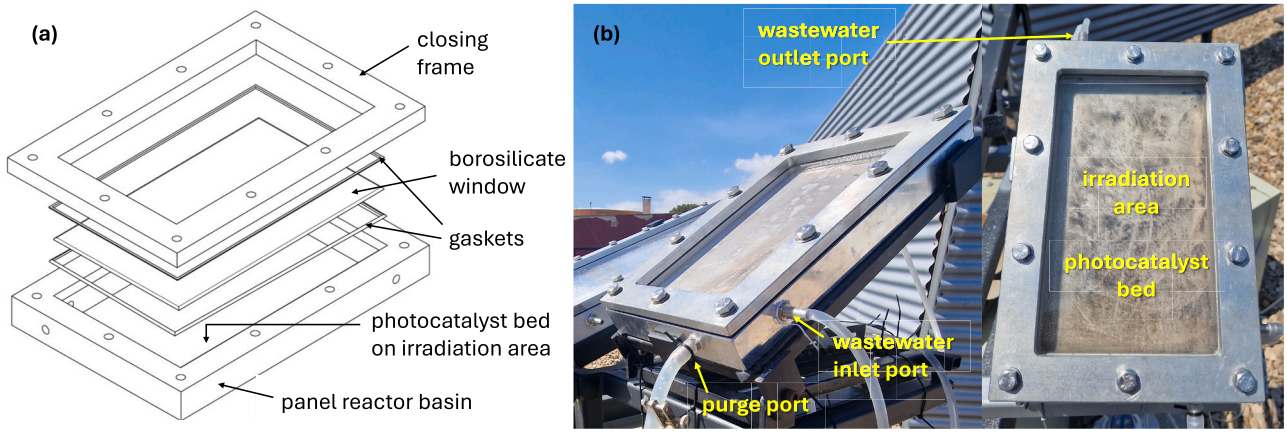

Fig. 1. (a) Schematic view of the parts and (b) photographs of the solar photocatalytic panel reactor used in this work.

3.2. Laboratory-scale screening of photocatalysts for H_2 production

3.2.1. Metal effect

The study on the effect of metal co-catalysts on hydrogen production performance was conducted using glucose as a model substrate, since it is a common monosaccharide and one of the structural blocks of sucrose, both present along with various other sugars in wastewaters from the food industry, such as those considered in this work. Both H_2 and CO_2 production were quantified as a measure of photoreforming efficiency and glucose oxidation and mineralisation in the photoreforming process (Table S5). The amounts of CO_2 produced are lower than those of H_2, but significant considering the expected reforming stoichiometry (H_2/CO_2 = 2:1). This indicates partial photoreforming of the glucose substrate [45–47], which undergoes stepwise degradation into lower oxygenates. The rates of CO_2 production are similar for Pt, Au, and Cu co-catalysts, whereas silver shows the lowest level of produced H_2 and CO_2, indicating that it exerts the lowest photoreforming activity.

Hydrogen production using photocatalysts containing different metals supported on TiO_2(P25) by deposition–precipitation ($^{DP}M/TiO_2$(P25); M = Cu, Ag, Au, Pt) is shown in Fig. 2a. A significant effect of the metal on hydrogen production can be observed. Platinum was the metal co-catalyst that achieved the highest production rate, consistent with similar studies in the literature [48–51]. The explanation for these results lies in the surface and catalytic properties of platinum. This noble metal is widely used in catalysis, especially in both hydrogenation and hydrogen evolution processes, since platinum enables a proper balance between adsorption and desorption, enhancing reaction kinetics [52,53]. Additionally, platinum is an excellent electron conductor, facilitating the rapid transfer of electrons to protons in the solution, thereby accelerating the initial stage of the reaction and minimizing energy losses [54]. For these reasons, Pt is selected as the reference metal for furnishing TiO_2 with co-catalytic function for subsequent photoreforming studies in this work.

3.2.2. Effect of platinum deposition method

The size of platinum particles can be a critical factor in determining the effectiveness of the co-catalyst. Smaller particles generally result in a higher surface-to-volume ratio, which increases the exposure of active sites. However, uneven distribution or particle agglomeration can reduce this efficiency [55]. The effect of Pt particles size on hydrogen production was evaluated (Fig. 2b). Under the reaction conditions used, it was found that the deposition method does not significantly impact the hydrogen production rate. The material that exhibited the highest production was $^{CR}Pt/TiO_2$(P25), with 4386 μmol H_2 g_{cat}^{-1}, although differences among the Pt/TiO_2(P25) series were small. This suggests that slight differences in particle sizes or particle size distributions have little impact on photocatalytic efficiencies, and that the remarkably high H_2 production rates in all cases are due to the intrinsic properties of platinum as a co-catalyst. Therefore, any of the evaluated deposition methods could be effectively employed for this application.

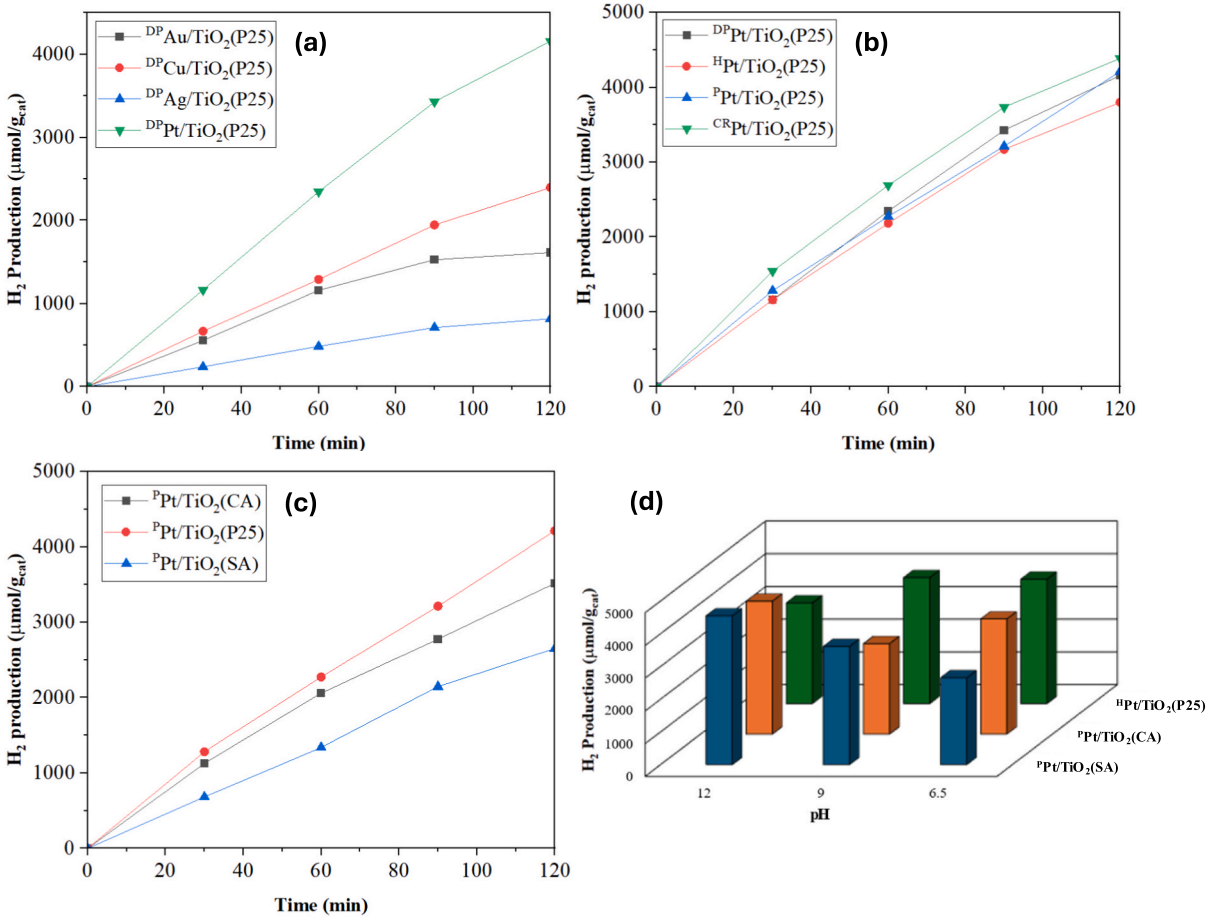

Fig. 2. Photocatalytic hydrogen production efficiency screening using glucose as the model substrate. (a) Effect of metal co-catalyst in $^{DP}M/TiO_2$(P25) (1 g L^{-1}; M: Cu, Ag, Au, Pt), showing that platinum is the most effective co-catalyst metal. (b) Impact of platinum deposition method in Pt/TiO_2(P25), revealing little or no influence. (c) Effect of the type of nanosized titania support in $^{P}Pt/TiO_2$, showing slightly better performance for the benchmark P25 anatase–rutile nanocomposite. (d) Effect of pH and nanosized titania support in selected Pt/TiO_2 photocatalysts, which points to higher H_2 evolution rates for $^{P}Pt/TiO_2$(SA) under increasingly basic conditions. Experimental conditions: Photocatalyst suspensions (1 g L^{-1}) in aqueous glucose (5 % w/v) under simulated sunlight (Xe lamp, AM1.5G, 1000 W m^{-2}) and nitrogen atmosphere.

3.2.3. TiO_2 type effect

The next step of this research was to assess the performance of different titanium dioxide nanosized supports as main photocatalyst semiconductor component on the photocatalytic hydrogen production on the Pt/TiO_2 derived therefrom. Hydrothermally synthesised anatase, commercial anatase and commercial anatase–rutile nanocomposite prepared by flame pyrolysis, namely TiO_2(SA), TiO_2(CA) and TiO_2(P25), respectively, were studied. Photodeposition was the chosen Pt loading method, as discussed above (Section 3.1.2).

Hydrogen production rates on $^{P}Pt/TiO_2$ were influenced by both the crystalline phase and the morphology of the support used (Fig. 2c). The highest H_2 production under the experimental conditions was observed for $^{P}Pt/TiO_2$(P25). The difference in activity between the $^{P}Pt/TiO_2$ photocatalysts based on P25 and commercial anatase is attributed to the anatase–rutile phase junction nanocomposite features of P25, which enhances charge separation, increases UV light absorption, and boosts the generation of reactive species, collectively resulting in higher photocatalytic activity [56–58]. On the other hand, $^{P}Pt/TiO_2$(SA) exhibited the lowest hydrogen production. This could be due to the reduced exposure of active sites caused by its aggregated microsphere morphology, as well as the surface property modifications induced by the carbon coating, which may affect the adsorption and interaction with organic species. It is also noteworthy that $^{P}Pt/TiO_2$(CA) and $^{P}Pt/TiO_2$(P25) led to similar CO_2 production rates, both noticeably higher than those recorded for $^{P}Pt/TiO_2$(SA), as evidenced in Table S5.

To evaluate the durability of the photocatalysts and the long-term photoreforming efficiency of the system, experiments were extended to continuous 24 h irradiation times using the $^{P}Pt/TiO_2$ materials (Fig. S9 and Table S6). Hydrogen production was rapid initially and then progressively slowed down upon prolonged irradiation after 2 h. Notwithstanding this, hydrogen evolution continued in a sustained trend, as revealed by the cumulative produced amounts after one day (around or exceeding 10 mmol g_{cat}^{-1}, Table S6). Explanation for such partial decline in activity has been related to the generation of oxidation intermediates that may bind to the photocatalyst surface [59], a phenomenon that is also expected to take place during the photoreforming of saccharides, as investigated herein. Nonetheless, the oxidation of such intermediates, most likely bearing carboxylate or other highly oxygenated moieties, does not lead to severe deactivation and, albeit more slowly, is expected to continue until complete photoreforming upon prolonged irradiation, as reported for similar systems [60,61]. This can be rationalised for glucose in our experiments by observing the overall decreasing H_2/CO_2 molar ratios at increasing reaction times (Table S6). These results indicate that, whilst hydrogen evolution prevails initially (most likely by dehydrogenation of CHOH moieties in glucose), more extensive oxidation ensues via consecutive reaction steps, eventually promoting mineralisation, as suggested by increasing CO_2 evolution. This sequence of oxidative events is consistent with previous detailed mechanistic studies [47,62].

3.2.4. pH effect

One of the physicochemical properties that most significantly affects photocatalytic hydrogen production rate is pH [12,63]. The pH of wastewaters from the food industry may vary along a wide range depending on the degradation or fermentation states of food ingredients or additives, and on the chemical agents employed in plant cleaning procedures. For this reason, the effect of pH changes on H_2 production was firstly evaluated for $^{P}Pt/TiO_2$(CA), $^{P}Pt/TiO_2$(SA) and $^{H}Pt/TiO_2$(P25) as a control, using glucose as a model substrate to provide a guide for photoreforming effectiveness for wastewater samples having pH values across wide ranges (Fig. 2d). At first glance, it is obvious that hydrogen production is significantly affected by both pH and the material used. In the case of $^{P}Pt/TiO_2$(SA), higher production efficiency is observed at pH = 12, while $^{H}Pt/TiO_2$(P25) shows a higher production rate at neutral conditions, and decreased activity as alkalinity increases. On the other hand, $^{P}Pt/TiO_2$(CA) does not exhibit a clear trend; although the lowest production occurs at pH = 9, it increases again in more basic media. As a general trend, anatase-based materials showed greater hydrogen production at pH = 12, while the P25-based counterpart reached its maximum production at pH ≤ 9.

Hydrogen production by photocatalytic wastewater treatment may be influenced by multiple factors, including the point of zero charge (PZC) of the photocatalyst, and in turn, the agglomeration of particles due to surface charges. If pH deviates from the PZC, the photocatalyst will agglomerate, and hence, adsorption of substrates will be hindered [64–66]. On the other hand, the protonation of the chemical agent, in this case, glucose, also plays a crucial role. At increasing pH, near or beyond the pK_a value of glucose (12.3), it will tend to deprotonate, facilitating its degradation due to more efficient reaction with holes, thereby increasing H_2 production [67,68], although electrostatic repulsion will impact negatively on efficiency. As mentioned above, previous studies, such as those conducted by Sanwald *et al.*, demonstrated that the photoreforming mechanism of glucose under neutral and acidic pH conditions involves the opening of aldose rings through the direct transfer of holes to chemisorbed oxygens [47]. This process generates primary formate esters, which are subsequently converted into intermediates via redox-neutral hydrolysis. This mechanism is expected to take place also under our experimental conditions, as proven by the detection of arabinose as a glucose oxidation intermediate (Fig. S10). Furthermore, alkalinisation enhances sustained H_2 production over time, primarily due to the rapid hydrolytic cleavage of formate intermediates induced by OH^- ions [47]. This is consistent with the higher hydrogen production observed herein at pH = 12 when using $^{P}Pt/TiO_2$(SA) and $^{P}Pt/TiO_2$(CA). Despite the lack of a clear trend in hydrogen production, which can be attributed to complex interactions of these phenomena, this study highlights the importance of selecting photocatalysts for wastewater treatment based on their pH to enhance photocatalytic efficiency and optimize hydrogen production. Consequently, given the wastewater samples studied herein (neutral to significantly basic), $^{P}Pt/TiO_2$(SA) and $^{H}Pt/TiO_2$(P25) were used aiming at high efficiency at high or slightly basic pH, down to levels close to neutrality.

3.3. Laboratory-scale hydrogen generation from juice production wastewaters

A laboratory-scale study was conducted with four different wastewater samples obtained from a fruit processing food production plant (physicochemical parameters described in Table S1). Despite having been sourced from the same plant, such parameters vary within wide ranges. Three out of the four wastewater samples (JWW2, JWW3 and JWW4) are noticeably basic, whilst one (JWW1) is almost neutral. Conductivities range between 800 and 4000 μS cm^{-1}. Organic matter contents are also varied, as reflected by their COD levels between 1000 and 7000 mg(O_2) L^{-1}. The observed diversity in wastewater characteristics represents a realistic scenario to assess the applicability prospects of photoreforming technologies.

The hydrogen production profiles for the different wastewaters using either $^{P}Pt/TiO_2$(SA) or $^{H}Pt/TiO_2$(P25) materials are shown in Fig. 3 and listed in Table S7. As observed, sustained hydrogen production was achieved from all the wastewater samples studied. Production rates were higher using $^{P}Pt/TiO_2$(SA) as compared to $^{H}Pt/TiO_2$(P25), except for JWW3. This partly correlates with the greater photocatalytic efficiency of the former material in alkaline pH conditions (Fig. 2d). The highest hydrogen productivity was observed for JWW4 using $^{P}Pt/TiO_2$(SA) as the photocatalyst, reaching a rate above 1.3 mmol(H_2) g_{cat}^{-1} h^{-1}. The difference in activity between $^{P}Pt/TiO_2$(SA) and $^{H}Pt/TiO_2$(P25) could be attributed to the carbon component present in the former (Section 3.1.1). Carboxylate groups in $^{P}Pt/TiO_2$(SA), as evidenced by FTIR (Fig. S6d), may increase surface affinity for organic molecules with functional groups such as the multiple hydroxyls in saccharides by means of hydrogen bonding in basic media, facilitating their adsorption and conversion. In general, the photocatalyst based on hydrothermally

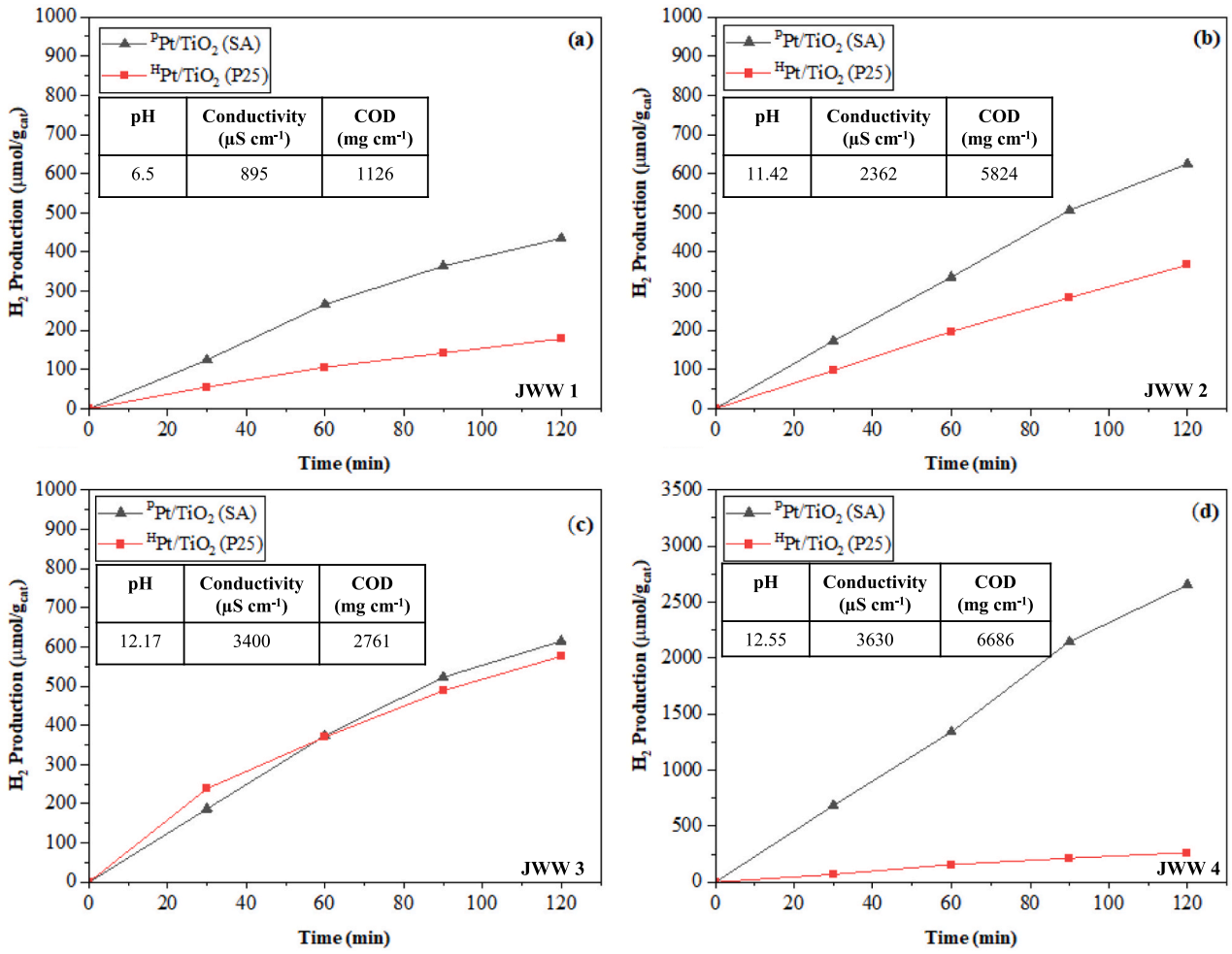

Fig. 3. Hydrogen production from different juice wastewaters: (a) JWW1, (b) JWW2, (c) JWW3 and (d) JWW4, using Pt/TiO_2 photocatalysts (1 g L^{-1}) under simulated sunlight (Xe lamp, AM1.5G, 1000 W m^{-2}) in laboratory-scale reactors. It is noteworthy that ^{P}Pt/TiO_2(SA) outperforms ^{P}Pt/TiO_2(P25), especially for effluents with high COD values and high saccharide contents. *i.e.* JWW2 and JWW4, as opposed to the trend observed for model neutral glucose solutions.

prepared carbon-containing titania showed a more robust performance at high pH.

Despite having similar physicochemical characteristics, different hydrogen production rates were observed for JWW3 and JWW4. In the case of JWW3, no significant difference in hydrogen production rate was observed between ^{P}Pt/TiO_2(SA) and ^{H}Pt/TiO_2(P25), suggesting that the difference in hydrogen production for JWW4 is not solely due to the pH of the solution but also possibly to the type and amount of dissolved organic matter. As shown in Table S1, JWW4 has 3.5 times higher COD than JWW3. It is important to note that in the photoreforming process using wastewater, dissolved organic matter acts as an electron donor for hydrogen production. Saccharides are known to behave as effective electron donors, and hence, as suitable substrates for photoreforming. Glucose is the most common monosaccharide, and has been considered in this work as the model substrate (see Section 3.2), showing favourable hydrogen production, especially under basic pH for ^{P}Pt/TiO_2(SA). The initial analyses of the wastewaters under study by HPLC reveals, in fact, that the concentration of glucose in JWW4 is sensibly higher (1442 mg L^{-1}, Table S2) than those in the other effluents. This is consistent with the highest hydrogen production observed for JWW4 using ^{P}Pt/TiO_2(SA) as the photocatalyst. A similar effect is evidenced, although to a lesser extent, for JWW2, which contains much lower an amount of glucose, but a noticeably high sucrose content (2295 mg L^{-1}, Table S2). The lower H_2 production rate, as compared to JWW4, on ^{P}Pt/TiO_2(SA) (625 *vs.* 2653 µmol g_{cat}^{-1} after 2 h irradiation times, Fig. 3 and Table S7) is probably a reflection of the more complex molecular structure of sucrose, a disaccharide, and its influence on photoreforming efficiencies. In other words, smaller and simpler oxygenated molecules tend to react faster and lead to higher hydrogen evolution rates. Other easily oxidizable organic substances not detected by HPLC can also consume of photogenerated holes, facilitating hydrogen production, for JWW1 and JWW3, which contain low amounts of glucose or sucrose. Further analyses will be performed on these and other wastewater samples to gain further insight into the structure–activity correlation regarding oxygenated substrates originated in food industries or other related activities. Overall, the gigantic diversity of possible contaminants constitutes an enormous challenge regarding mechanistic and efficiency investigations of photoreforming processes. In addition, some organic molecules may also compete with H^+ for electrons during the reduction reaction, potentially inhibiting the efficiency of hydrogen evolution [69].

Additionally, it should be mentioned that in the experiments using highly basic juice production wastewaters (JWW2, JWW3 and JWW4), low productivities of CO_2 were recorded in the gas phase ($\leq$10 µmol g_{cat}^{-1} h^{-1}, Table S7), since it would remain absorbed in the form of carbonate/bicarbonate in the aqueous media due to their alkaline pH values. Conversely, the highest CO_2 production rate for the neutral JWW1 was recorded using ^{P}Pt/TiO_2(SA) as the photocatalyst.

In addition to gas production, the physicochemical evolution of the wastewaters was studied by post-photocatalysis analyses. Changes in the

physicochemical properties of the wastewaters were observed after photoreforming under simulated sunlight. In general, decreases in pH and conductivity were observed (Fig. S11), most likely owing to the degradation of organic matter into organic acid intermediates, and eventually, into carbon dioxide. Such oxidation products partly neutralize the initial alkaline species, hence lowering the pH of the solution. Regarding conductivity, slight increases were observed for JWW1, whereas noticeable decreases took place for the basic JWW2–4 samples. High pH values in the latter are due to the presence of caustic substances, most likely sodium hydroxide, used for pipe cleaning operations at the food processing plant. Hence, the lowered conductivity could be due to a combination of partial neutralisation of hydroxide by acidic intermediates formed during the oxidative reaction steps inherent to the photoreforming of saccharides, as discussed above, and to the formation of larger anions as by-products, such as carbonate, bicarbonate or a range of possible carboxylate-containing species. Finally, the slight increases in the conductivity of the nearly basic JWW1 might be ascribed to the formation of ionisable intermediates such as acids of low molecular weight, e.g. formic or lactic. The greatest change in pH and conductivity was observed for JWW4 on $^{P}Pt/TiO_2$(SA), consistent with the also higher hydrogen production results obtained in that case.

3.4. *Pre-pilot-scale photoreforming of juice production wastewaters in a solar panel reactor*

Outdoors photoreforming experiments under natural sunlight were performed in a flat panel reactor (see Section 2.6). A long-term solar photoreforming experiment was performed using JWW2 as the wastewater substrate and $^{H}Pt/TiO_2$(P25) as the photocatalyst. This wastewater sample was selected based on reasonable hydrogen production efficiency in laboratory-scale experiments, and on its moderate pH, which is lower than those of JWW3 and JWW4, since highly caustic

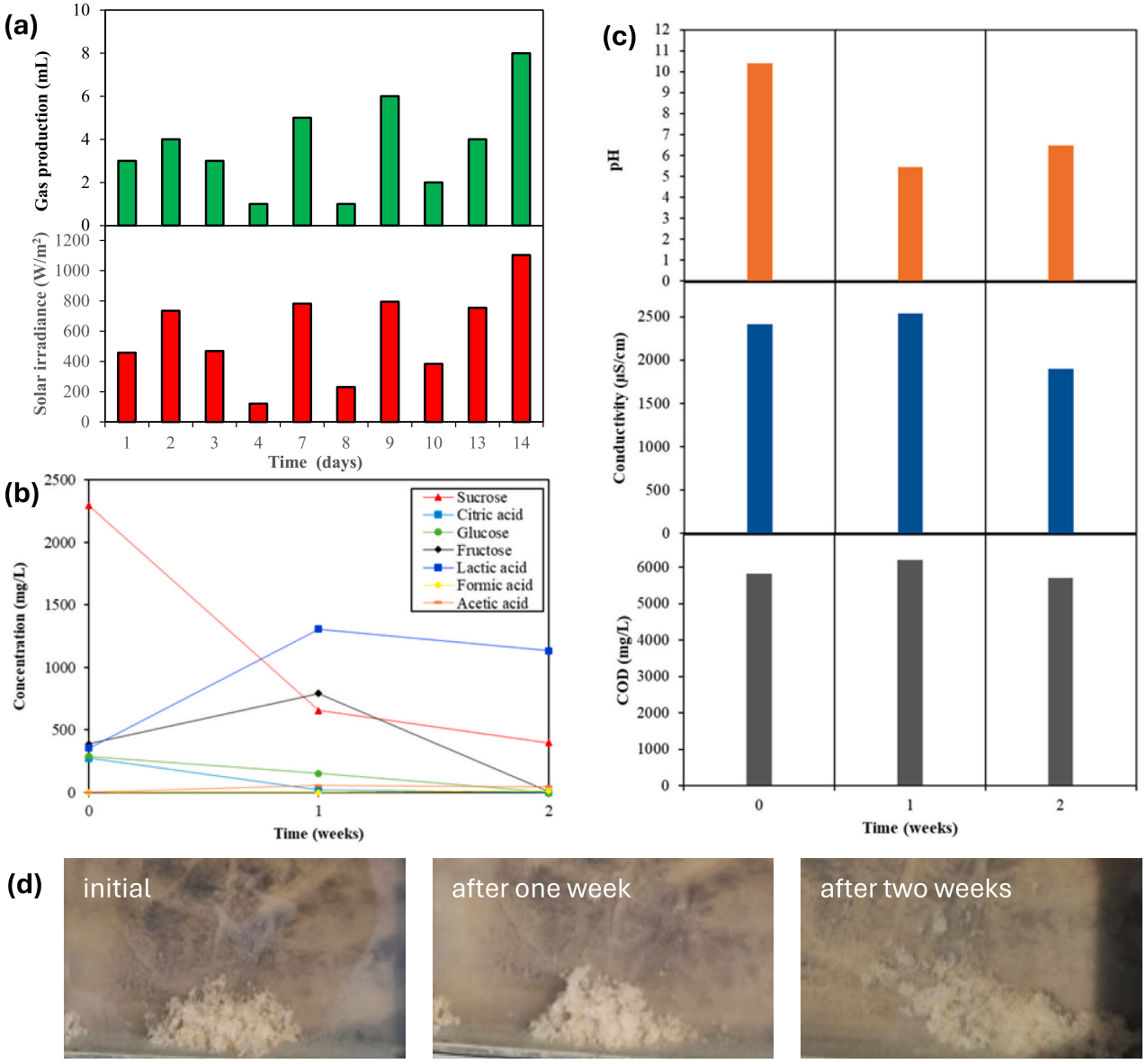

Fig. 4. Main results of outdoors pre-pilot photoreforming of juice production wastewater in a panel reactor under natural sunlight over the course of two weeks. (a) Correlation between daily gas production and solar irradiance, confirming their direct cause-effect relationship. (b) Evolution of the amounts of main oxygenated substances, determined by HPLC, showing effective saccharide conversion and transient formation of lactate and fructose interediates. (c) Evolution of physicochemical wastewater parameters; the main trends observed are rapid pH decrease, slower conductivity decrease and little change in COD (see text for details). (d) Evolution of solid sediment in the panel reactor. Photocatalytic panel parameters: continuous treatment of a wastewater sample (JWW2, 1.5 L) under natural sunlight irradiation (2 weeks, July/2023), 14 × 24 cm irradiated area (0.033 m^2), $^{H}Pt/TiO_2$ deposited by solvent casting (*ca.* 10 g m^{-2}).

aqueous effluents were observed to lead to corrosion of some exposed aluminium parts of the panel. Remarkably, the correlation between gas production volumes and solar irradiances recorded for different days is clearly noteworthy (Fig. 4a and Table S8). The weather for initial days was variable and cloudier in general, as illustrated by highly disperse (but lower on average) irradiances, resulting in obvious fluctuation in gas production volumes, ranging from 1 to 6 mL per day, followed by a general increase on latter days. Particularly, on days 7, 9 and 14, which were sunnier, in accordance with stronger irradiance, the volumes of gas produced were also highest, peaking at 8 mL on the last day. This suggests that higher solar intensity enhances the photocatalytic activity of the $^{H}Pt/TiO_2$(P25) catalyst, resulting in greater hydrogen production. Evolution rates of gaseous products achieved remarkable values on those days, equating to > 100 μmol g^{-1} h^{-1}, *i.e.* > 1000 μmol m^{-2} h^{-1} (see Table S8). Although lower than the efficiencies observed in laboratory-scale experiments, these results are encouraging considering they represent a first attempt. Nonetheless, improvements in the panel system must be achieved in future development to attain competitive hydrogen yields. Analysis of the produced gases revealed low H_2/CO_2 molar ratios (0.2–0.3 for days 9 and 14, Table S8), indicative of high mineralisation and/or decarboxylation degrees after long solar irradiation periods.

The degradation of oxygenated substances, chiefly saccharides and organic acids, in the juice production wastewater studied (JWW2) was monitored by HPLC (Fig. 4b). It should be noted that the analysed acids are likely to have been in their deprotonated forms (carboxylates) in the wastewater medium due to its alkaline or neutral pH. The specific compounds initially contained in the wastewater sample were sucrose, citric acid, glucose, fructose and lactic acid, whereas minor amounts of formic acid and acetic acid were also detected upon irradiation. The pre-pilot-scale photocatalytic panel reactor treatment effectively resulted in the degradation of several key carbohydrates, particularly sucrose, citric acid, glucose, and fructose. The results indicate substantial reduction in these compounds within two weeks, with nearly complete degradation of citric acid and glucose. Notably, fructose exhibited an initial increase after one week, possibly due to intermediate scission of sucrose or other oligosaccharides, before subsequent degradation during the second week. The increasing levels of lactic, formic and acetic acids after the first week suggest the formation of these compounds as by-products of the degradation process. Nonetheless, continued irradiation led to overall degradation of all oxygenated substances, as evidenced by their consistently decreasing levels after the second week of solar photoreforming.

The effect of outdoors solar photoreforming on the physicochemical parameters of the juice production wastewater employed in the panel reactor using $^{H}Pt/TiO_2$(P25) as a catalyst is noteworthy, as shown in Fig. 4c. The significant decrease in pH within the first week (from 10.4 to 5.4) indicates the formation of acidic by-products and ultimately CO_2, consistent with the significant degradation of sucrose, citric acid, and glucose. The increase in lactic acid and initial formation of formic and acetic acids (Fig. 4b) support the observation of acidification. In general, degradation of oxygenated species via photoreforming results in the release of protic species [12]. The subsequent slight increase in pH by the second week (from 5.4 to 6.5) suggests partial neutralisation: further degradation of organic acids, chiefly lactic, and eventual release of CO_2 into the gas phase, align with pH stabilisation. Although the formation of formic and acetic acids continues, it does not significantly impact pH due to their low concentrations. The conductivity results indicate dynamic changes in the ionic content of the wastewater, with an initial slight increase (from 2.4 to 2.5 mS cm^{-1} after 1 week) followed by a substantial decrease (1.9 mS cm^{-1} after 2 weeks), reflecting the complex nature of ionic species formation and degradation during treatment. Moreover, COD measurements showed an initial increase from 5.8 to 6.8 g(O_2) L^{-1} after the first week, possibly due to partial water evaporation and/or to the breakdown of solids into soluble intermediates, followed by a reduction to 5.7 mg(O_2) L^{-1} after the second week, suggesting effective but still incomplete degradation of organic matter. Even if the results collectively indicate (based on H_2/CO_2 evolution, and pH and conductivity decrease) that photoreforming is taking place, the extent of degradation is not substantial according to the obtained COD data. Current and future work in our pilot system is focused on intensifying reduction of organic matter by enlarging irradiation areas and improving overall photocatalytic activity.

The wastewaters employed in this study were not pretreated by any physical means. Some insoluble, most likely fibrous, material was initially present in the JWW2 sample used for the natural sunlight photoreforming experiment in the panel reactor. The solids were mostly settled on the bottom of the reservoir tank at the beginning of the experiment. Part of these solids were accidentally carried over to the irradiated basin of the panel reactor, covering a small area of the photocatalyst bed (Fig. 4d). The evolution of these solids was monitored as a way to study their behaviour during solar photoreforming and their effect on the photoreforming experiment. At the initial stage (a), the solids appear as dense and cohesive aggregates, indicating that the organic matter and particulates in the juice wastewater were still intact. After one week of treatment, the size and aggregation state of the solids seems to decrease, with visible fragmentation. This suggests partial breakdown of larger particles, likely due to the photocatalytic degradation of complex organic compounds facilitated by the $^{H}Pt/TiO_2$(P25) catalyst. By the end of the second week, the solid content was further diminished, as indicated by the much smaller and more dispersed aggregates observed. This slight reduction in size and concentration of solids represents a qualitative indication of partial solids disintegration. The important evolution of solids will be studied for prolonged periods in subsequent experiments. It is important to note that no additional solids emerge during the experiment, and hence, sludge production is inhibited under the anaerobic conditions of the solar photocatalytic experiment. This beneficial aspect aligns with the overall degradation of organic matter, as confirmed by the observed gas production and decreases in pH and conductivity.

This demonstrative photocatalytic experiment under natural sunlight demonstrates the effectiveness of solar photoreforming in panel reactors as a promising alternative wastewater treatment technology. Sustained and consistent gas production has been recorded along with simultaneous degradation of organic contaminants in wastewaters from the manufacture of processed food, mainly from fruit ingredients. Ample possibilities might be envisaged for other wastewater types, in combination with on-purpose designed photocatalysts.

4. Conclusions

Motivated by the ultimate goal of demonstrating solar photoreforming for the valorisation of food industry wastewaters, enabling the production of hydrogen, the transition from laboratory experiments to a solar photocatalytic panel has been investigated herein. Specifically, wastewater effluents from a plant manufacturing processed food (mainly fruit) products have been used as the substrate. Initial optimisation of metal/titania (M/TiO_2; *M*: Cu, Ag, Au or Pt) photocatalysts was performed using glucose as the substrate, at varying pH, and under simulated sunlight. Platinum was the best performing co-catalyst, followed by copper and gold. A dedicated study of different nanosized titania supports indicated that the commercial anatase–rutile benchmark (P25), produced by flame pyrolysis, exhibits superior hydrogen production efficiency under neutral conditions. Conversely, Pt-loaded pure-phase anatase performs better under basic conditions; remarkable activity (> 4.5 mmol(H_2) g_{cat}^{-1} h^{-1}, for $c_{glucose} = 5$ % *w/v*, pH = 12, simulated sunlight) was achieved for hydrothermally synthesised titania with a partly oxidised carbonaceous coating, with photodeposited platinum, *i.e.* $^{P}Pt/TiO_2$(SA). This might be due to increased surface affinity of pending carboxylate groups on the surface of TiO_2(SA) for organic molecules with multiple hydroxyls, *e.g.* saccharides, in basic media, facilitating their adsorption and conversion. Importantly, the

highest hydrogen production activity was also observed for highly basic wastewaters using $^{P}Pt/TiO_2$(SA) as the photocatalyst (> 1.3 mmol(H_2) g_{cat}^{-1} h^{-1}, pH > 12.5).

Food industry wastewater treatment has been proven under natural sunlight in a novel solar panel reactor. By recirculating such complex aqueous effluent on the photocatalyst bed for two weeks, its main parameters improved regarding quality and discharge regulations. Decreases were observed for pH (from *ca.* 11 to < 6) and conductivity (from 2.4 to 1.9 mS cm^{-1}), whereas saccharides were degraded into simpler oxygenates and eventually mineralised to carbon dioxide, and solids tended to disintegrate. Importantly, daily gas production volumes were remarkably parallel to sunlight irradiance. Although the obtained results are preliminary and a long optimisation and development path lies ahead, the demonstration presented herein is encouraging for the consideration of solar photocatalysis as a serious valorisation alternative to current wastewater treatment technologies, which are mostly destructive, energy-consuming and complex.

CRediT authorship contribution statement

Laura Carolina Valencia-Valero: Writing – original draft, Methodology, Investigation, Formal analysis, Data curation. **Kevin A. Simbaña:** Methodology, Investigation, Formal analysis, Data curation. **Jonas E. Eleraky:** Methodology, Investigation, Formal analysis, Data curation. **Monika Hapońska:** Writing – original draft, Supervision, Methodology, Investigation, Formal analysis, Data curation. **Alberto Puga:** Writing – review & editing, Validation, Supervision, Resources, Project administration, Methodology, Investigation, Funding acquisition, Formal analysis, Data curation, Conceptualization.

Declaration of competing interest

The authors declare the following financial interests/personal relationships which may be considered as potential competing interests: Alberto Puga reports financial support was provided by State Agency of Research. If there are other authors, they declare that they have no known competing financial interests or personal relationships that could have appeared to influence the work reported in this paper.

Acknowledgments

This publication is part of the projects TED2021-129496B-I00 and CPP2021-008619, funded by the Spanish Research State Agency (MICIU/AEI/10.13039/501100011033) and the European Union (NextGenerationEU/PRTR). The partners of the latter grant, namely FACSA, ENAGÁS, and *Eurecat Centre Tecnològic*, and additional collaborating entities, namely *Consorci Besòs Tordera*, *Transparenta*® and the wastewater treatment plant managed by them in Granollers (EDAR Granollers, Barcelona, Spain) are also gratefully acknowledged for their ongoing support to our investigations. We sincerely thank the headquarters of Delafruit S.L.U. (Tarragona, Spain), a healthy food manufacturer, for supplying wastewater samples and providing valuable information, in addition to expressing their interest in these investigations. L.C.V.V. thanks Universitat Rovira i Virgili for a predoctoral contract (2021PMF-PIPF-15) within its *Marti i Franquès* programme.

Appendix A. Supplementary data

Supplementary data to this article can be found online at https://doi.org/10.1016/j.cej.2025.161636.

Data availability

Data will be made available on request.

References

[1] M. Qadir, P. Drechsel, B. Jiménez Cisneros, Y. Kim, A. Pramanik, P. Mehta, O. Olaniyan, Global and regional potential of wastewater as a water, nutrient and energy source, Nat. Res. Forum 44 (2020) 40–51, https://doi.org/10.1111/1477-8947.12187.
[2] B. Pratap, S. Kumar, S. Nand, I. Azad, R.N. Bharagava, L.F. Romanholo Ferreira, V. Dutta, Wastewater generation and treatment by various eco-friendly technologies: Possible health hazards and further reuse for environmental safety, Chemosphere 313 (2023) 137547, https://doi.org/10.1016/j.chemosphere.2022.137547.
[3] D.L. Russell, Practical wastewater treatment, Wiley-Interscience, Hoboken, 2006.
[4] H. Chen, O.A. Ahmed, P.K. Singh, B.S. Abdullaeva, M. Alhadrawi, Y. Elmasry, M. S. Safi, I. Mahariq, Coupling a thermoelectric-based heat recovery and hydrogen production unit with a SOFC-powered multi-generation structure; an in-depth economic machine learning-driven analysis, Case Stud. Therm. Eng. 61 (2024) 105046, https://doi.org/10.1016/j.csite.2024.105046.
[5] S.S. Tak, O. Shetye, O. Muley, H. Jaiswal, S.N. Malik, Emerging technologies for hydrogen production from wastewater, Int. J. Hydrogen Energy 47 (2022) 37282–37301, https://doi.org/10.1016/j.ijhydene.2022.06.225.
[6] Global Hydrogen Review 2023, (2023).
[7] S.C. Wijayasekera, K. Hewage, O. Siddiqui, P. Hettiaratchi, R. Sadiq, Waste-to-hydrogen technologies: A critical review of techno-economic and socio-environmental sustainability, Int. J. Hydrogen Energy 47 (2022) 5842–5870, https://doi.org/10.1016/j.ijhydene.2021.11.226.
[8] J. Lui, W.-H. Chen, D. Tsang, S. You, A critical review on the principles, applications, and challenges of waste-to-hydrogen technologies, Renew. Sustain. Energy Rev. 134 (2020) 110365, https://doi.org/10.1016/j.rser.2020.110365.
[9] H. Lin, M. Zhang, B.S. Chauhan, H. Ayed, M.A. Khadimallah, X. Tang, I. Mahariq, Development, kinetic analysis, and economic feasibility of different Corn Stover-driven biorefineries to produce biohydrogen, bioethanol, and biomethane: A comparative analysis, Renew. Energy 237 (2024) 121625, https://doi.org/10.1016/j.renene.2024.121625.
[10] G. Lopez, M. Artetxe, M. Amutio, J. Alvarez, J. Bilbao, M. Olazar, Recent advances in the gasification of waste plastics. A critical overview, Renew. Sustain. Energy Rev. 82 (2018) 576–596, https://doi.org/10.1016/j.rser.2017.09.032.
[11] R.M. Navarro, M.C. Sánchez-Sánchez, M.C. Alvarez-Galvan, F.D. Valle, J.L. G. Fierro, Hydrogen production from renewable sources: biomass and photocatalytic opportunities, Energy Environ. Sci. 2 (2009) 35–54, https://doi.org/10.1039/B808138G.
[12] A.V. Puga, Photocatalytic production of hydrogen from biomass-derived feedstocks, Coord. Chem. Rev. 315 (2016) 1–66, https://doi.org/10.1016/j.ccr.2015.12.009.
[13] T.H. Jeon, M.S. Koo, H. Kim, W. Choi, Dual-Functional Photocatalytic and Photoelectrocatalytic Systems for Energy- and Resource-Recovering Water Treatment, ACS Catal. 8 (2018) 11542–11563, https://doi.org/10.1021/acscatal.8b03521.
[14] K. Shimura, H. Yoshida, Heterogeneous photocatalytic hydrogen production from water and biomass derivatives, Energy Environ. Sci. 4 (2011) 2467–2481, https://doi.org/10.1039/C1EE01120K.
[15] S.S. Mani, S. Rajendran, T. Mathew, C.S. Gopinath, A review on the recent advances in the design and structure–activity relationship of TiO_2 -based photocatalysts for solar hydrogen production, Energy Adv. 3 (2024) 1472–1504, https://doi.org/10.1039/D4YA00249K.
[16] Y. Ma, X. Wang, Y. Jia, X. Chen, H. Han, C. Li, Titanium Dioxide-Based Nanomaterials for Photocatalytic Fuel Generations, Chem. Rev. 114 (2014) 9987–10043, https://doi.org/10.1021/cr500008u.
[17] Q. Guo, C. Zhou, Z. Ma, X. Yang, Fundamentals of TiO_2 photocatalysis: Concepts, mechanisms, and challenges, Adv. Mater. 31 (2019) 1901997, https://doi.org/10.1002/adma.201901997.
[18] X. Chen, S.S. Mao, Titanium Dioxide Nanomaterials: Synthesis, Properties, Modifications, and Applications, Chem. Rev. 107 (2007) 2891–2959, https://doi.org/10.1021/cr0500535.
[19] J. Schneider, M. Matsuoka, M. Takeuchi, J. Zhang, Y. Horiuchi, M. Anpo, D. W. Bahnemann, Understanding TiO_2 photocatalysis: Mechanisms and materials, Chem. Rev. 114 (2014) 9919–9986, https://doi.org/10.1021/cr5001892.
[20] J. Yang, D. Wang, H. Han, C. Li, Roles of Cocatalysts in Photocatalysis and Photoelectrocatalysis, Acc. Chem. Res. 46 (2013), https://doi.org/10.1021/ar300227e.
[21] J. Ran, J. Zhang, J. Yu, M. Jaroniec, S.Z. Qiao, Earth-abundant cocatalysts for semiconductor-based photocatalytic water splitting, Chem. Soc. Rev. 43 (2014) 7787–7812, https://doi.org/10.1039/C3CS60425J.
[22] S. Bhattacharjee, S. Linley, E. Reisner, Solar reforming as an emerging technology for circular chemical industries, Nat Rev Chem 8 (2024) 87–105, https://doi.org/10.1038/s41570-023-00567-x.
[23] A. Rioja-Cabanillas, D. Valdesueiro, P. Fernandez-Ibanez, J. Byrne, Hydrogen from wastewater by photocatalytic and photoelectrochemical treatment, Journal of Physics: Energy 3 (2020), https://doi.org/10.1088/2515-7655/abceab.
[24] C. Yan, A. Basem, H.A. Al-Asadi, M.A. Alghassab, X. Zhou, S. Shomurotova, D. J. Jasim, I. Albaijan, H.F. Alotaibi, M. Alhadrawi, I. Mahariq, Novel $Fe_2O_3/Bi_2O_3/CeO_2$ heterojunction photocatalyst for wastewater treatment: characterization, photocatalytic performance and mechanism study, J. Mol. Liq. 410 (2024) 125580, https://doi.org/10.1016/j.molliq.2024.125580.
[25] H. Luo, J. Barrio Hermida, N. Sunny, A. Li, L. Steier, N. Shah, I. Stephens, M. Titirici, Progress and Perspectives in Photo- and Electrochemical-Oxidation of

Biomass for Sustainable Chemicals and Hydrogen Production, Adv. Energy Mater. 11 (2021) 2101180, https://doi.org/10.1002/aenm.202101180.
[26] C.Y. Toe, C. Tsounis, J. Zhang, H. Masood, D. Gunawan, J. Scott, R. Amal, Advancing photoreforming of organics: highlights on photocatalyst and system designs for selective oxidation reactions, Energy Environ. Sci. 14 (2021) 1140–1175, https://doi.org/10.1039/D0EE03116J.
[27] K. Villa, X. Domènech, S. Malato, M.I. Maldonado, J. Peral, Heterogeneous photocatalytic hydrogen generation in a solar pilot plant, Int. J. Hydrogen Energy 38 (2013) 12718–12724, https://doi.org/10.1016/j.ijhydene.2013.07.046.
[28] S.Y. Arzate Salgado, R.M. Ramírez Zamora, R. Zanella, J. Peral, S. Malato, M. I. Maldonado, Photocatalytic hydrogen production in a solar pilot plant using a Au/TiO_2 photo catalyst, Int. J. Hydrogen Energy 41 (2016) 11933–11940, https://doi.org/10.1016/j.ijhydene.2016.05.039.
[29] J.G. Villachica-Llamosas, A. Ruiz-Aguirre, G. Colón, J. Peral, S. Malato, CuO–TiO_2 pilot-plant system performance for solar photocatalytic hydrogen production, Int. J. Hydrogen Energy 51 (2024) 1069–1077, https://doi.org/10.1016/j.ijhydene.2023.07.149.
[30] M. Imizcoz, A.V. Puga, Assessment of photocatalytic hydrogen production from biomass or wastewaters depending on the metal Co-catalyst and Its deposition method on TiO_2, Catalysts 9 (2019) 584, https://doi.org/10.3390/catal9070584.
[31] A. Speltini, M. Sturini, F. Maraschi, D. Dondi, G. Fisogni, E. Annovazzi, A. Profumo, A. Buttafava, Evaluation of UV-A and solar light photocatalytic hydrogen gas evolution from olive mill wastewater, Int. J. Hydrogen Energy 40 (2015) 4303–4310, https://doi.org/10.1016/j.ijhydene.2015.01.182.
[32] A. Speltini, F. Gualco, F. Maraschi, M. Sturini, D. Dondi, L. Malavasi, A. Profumo, Photocatalytic hydrogen evolution assisted by aqueous (waste)biomass under simulated solar light: Oxidized g-C_3N_4 vs. P25 titanium dioxide, Int. J. Hydrogen Energy 44 (2019) 4072–4078, https://doi.org/10.1016/j.ijhydene.2018.12.126.
[33] Y. Li, L. Kuang, D. Xiao, A.R. Badireddy, M. Hu, S. Zhuang, X. Wang, E.S. Lee, T. Marhaba, W. Zhang, Hydrogen production from organic fatty acids using carbon-doped TiO_2 nanoparticles under visible light irradiation, Int. J. Hydrogen Energy 43 (2018) 4335–4346, https://doi.org/10.1016/j.ijhydene.2018.01.042.
[34] L. Liu, D.M. Meira, R. Arenal, P. Concepcion, A.V. Puga, A. Corma, Determination of the Evolution of Heterogeneous Single Metal Atoms and Nanoclusters under Reaction Conditions: Which Are the Working Catalytic Sites? ACS Catal. 9 (2019) 10626–10639, https://doi.org/10.1021/acscatal.9b04214.
[35] S. Chen, Q. Yang, H. Wang, S. Zhang, J. Li, Y. Wang, W. Chu, Q. Ye, L. Song, Initial Reaction Mechanism of Platinum Nanoparticle in Methanol–Water System and the Anomalous Catalytic Effect of Water, Nano Lett. 15 (2015) 5961–5968, https://doi.org/10.1021/acs.nanolett.5b02098.
[36] J. Quinson, J. Bucher, S.B. Simonsen, L.T. Kuhn, S. Kunz, M. Arenz, Monovalent Alkali Cations: Simple and Eco-Friendly Stabilizers for Surfactant-Free Precious Metal Nanoparticle Colloids, ACS Sustainable Chem. Eng. 7 (2019) 13680–13686, https://doi.org/10.1021/acssuschemeng.9b00681.
[37] A. Puga, D. Fattoruso, Photocatalytic panel reactor for the anaerobic photoreforming of waste aqueous effluents and the production of hydrogen as co-product, Eur. Pat. 4129931 (2023) A1.
[38] B. Liu, L.-M. Liu, X.-F. Lang, H.-Y. Wang, X.W. Lou, E.S. Aydil, Doping high-surface-area mesoporous TiO_2 microspheres with carbonate for visible light hydrogen production, Energy Environ. Sci. 7 (2014) 2592–2597, https://doi.org/10.1039/c4ee00472h.
[39] H. Li, X. Zhang, X. Cui, A Facile and Waste-Free Strategy to Fabricate Pt-C/TiO_2 Microspheres: Enhanced Photocatalytic Performance for Hydrogen Evolution, International Journal of Photoenergy 2014 (2014) e414281, https://doi.org/10.1155/2014/414281.
[40] Z. He, W. Que, J. Chen, Y. He, G. Wang, Surface chemical analysis on the carbon-doped mesoporous TiO_2 photocatalysts after post-thermal treatment: XPS and FTIR characterization, J. Phys. Chem. Solid 74 (2013) 924–928, https://doi.org/10.1016/j.jpcs.2013.02.001.
[41] M.A. Mohamed, W.N.W. Salleh, J. Jaafar, Z.A. Mohd Hir, M.S. Rosmi, M. Abd, A. F. Mutalib, M.T. Ismail, Regenerated cellulose membrane as bio-template for in-situ growth of visible-light driven C-modified mesoporous titania, Carbohydr. Polym. 146 (2016) 166–173, https://doi.org/10.1016/j.carbpol.2016.03.050.
[42] A.V. Puga, N. Barka, M. Imizcoz, Simultaneous H_2 production and bleaching via solar photoreforming of model Dye-polluted wastewaters on Metal/Titania, ChemCatChem 13 (2021) 1513–1529, https://doi.org/10.1002/cctc.202001048.
[43] Z.H.N. Al-Azri, M. AlOufi, A. Chan, G.I.N. Waterhouse, H. Idriss, Metal Particle Size Effects on the Photocatalytic Hydrogen Ion Reduction, ACS Catal. 9 (2019) 3946–3958, https://doi.org/10.1021/acscatal.8b05070.
[44] C. Dessal, L. Martínez, C. Maheu, T. Len, F. Morfin, J.L. Rousset, E. Puzenat, P. Afanasiev, M. Aouine, L. Soler, J. Llorca, L. Piccolo, Influence of Pt particle size and reaction phase on the photocatalytic performances of ultradispersed Pt/TiO_2 catalysts for hydrogen evolution, J. Catal. 375 (2019) 155–163, https://doi.org/10.1016/j.jcat.2019.05.033.
[45] E. Bahadori, G. Ramis, D. Zanardo, F. Menegazzo, M. Signoretto, D. Gazzoli, D. Pietrogiacomi, A.D. Michele, I. Rossetti, Photoreforming of glucose over CuO/TiO_2, Catalysts 10 (2020) 477, https://doi.org/10.3390/catal10050477.
[46] M. Bellardita, E.I. García-López, G. Marcì, G. Nasillo, L. Palmisano, Photocatalytic solar light H_2 production by aqueous glucose reforming, Eur. J. Inorg. Chem. 2018 (2018) 4522–4532, https://doi.org/10.1002/ejic.201800663.
[47] K.E. Sanwald, T.F. Berto, W. Eisenreich, A. Jentys, O.Y. Gutiérrez, J.A. Lercher, Overcoming the rate-limiting reaction during photoreforming of sugar aldoses for H_2-generation, ACS Catal. 7 (2017) 3236–3244, https://doi.org/10.1021/acscatal.7b00508.
[48] G.R. Bamwenda, S. Tsubota, T. Nakamura, M. Haruta, Photoassisted hydrogen production from a water-ethanol solution: a comparison of activities of Au-TiO_2 and Pt-TiO_2, J. Photochem. Photobiol. A Chem. 89 (1995) 177–189, https://doi.org/10.1016/1010-6030(95)04039-I.
[49] Z.H.N. Al-Azri, W.-T. Chen, A. Chan, V. Jovic, T. Ina, H. Idriss, G.I.N. Waterhouse, The roles of metal co-catalysts and reaction media in photocatalytic hydrogen production: Performance evaluation of M/TiO_2 photocatalysts (M = Pd, Pt, Au) in different alcohol–water mixtures, J. Catal. 329 (2015) 355–367, https://doi.org/10.1016/j.jcat.2015.06.005.
[50] Y.Z. Yang, C.-H. Chang, H. Idriss, Photo-catalytic production of hydrogen form ethanol over M/TiO_2 catalysts (M = Pd, Pt or Rh), Appl Catal B 67 (2006) 217–222, https://doi.org/10.1016/j.apcatb.2006.05.007.
[51] F.J. López-Tenllado, J. Hidalgo-Carrillo, V. Montes, A. Marinas, F.J. Urbano, J. M. Marinas, L. Ilieva, T. Tabakova, F. Reid, A comparative study of hydrogen photocatalytic production from glycerol and propan-2-ol on M/TiO_2 systems (M=Au, Pt, Pd), Catal. Today 280 (2017) 58–64, https://doi.org/10.1016/j.cattod.2016.05.009.
[52] T. Brülle, A. Denisenko, H. Sternschulte, U. Stimming, Catalytic activity of platinum nanoparticles on highly boron-doped and 100-oriented epitaxial diamond towards HER and HOR, PCCP 13 (2011) 12883–12891, https://doi.org/10.1039/C1CP20852G.
[53] L. Farzaneh, A.N. Pour, A DFT study of hydrogen adsorption on metallic platinum: Associative or dissociative adsorption, (2022). https://doi.org/10.21203/rs.3.rs-1494704/v1.
[54] D. Jiang, S. Overbury, S. Dai, Structures and energetics of Pt clusters on TiO_2: Interplay between metal-metal bonds and metal-oxygen bonds, J. Phys. Chem. C 116 (2012), https://doi.org/10.1021/jp3072102.
[55] B.R. Cuenya, Synthesis and catalytic properties of metal nanoparticles: Size, shape, support, composition, and oxidation state effects, Thin Solid Films 518 (2010) 3127–3150, https://doi.org/10.1016/j.tsf.2010.01.018.
[56] H.N.C. Dharma, J. Jaafar, N. Widiastuti, H. Matsuyama, S. Rajabsadeh, M.H. D. Othman, M.A. Rahman, N.N.M. Jafri, N.S. Suhaimin, A.M. Nasir, N.H. Alias, A review of titanium dioxide (TiO_2)-based photocatalyst for oilfield-produced water treatment, Membranes (basel) 12 (2022) 345, https://doi.org/10.3390/membranes12030345.
[57] A. Mishra, A. Mehta, S. Basu, Clay supported TiO_2 nanoparticles for photocatalytic degradation of environmental pollutants: A review, J. Environ. Chem. Eng. 6 (2018) 6088–6107, https://doi.org/10.1016/j.jece:2018.09.029.
[58] D.O. Scanlon, C.W. Dunnill, J. Buckeridge, S.A. Shevlin, A.J. Logsdail, S. M. Woodley, C.R.A. Catlow, M.J. Powell, R.G. Palgrave, I.P. Parkin, G.W. Watson, T.W. Keal, P. Sherwood, A. Walsh, A.A. Sokol, Band alignment of rutile and anatase TiO_2, Nature Mater 12 (2013) 798–801, https://doi.org/10.1038/nmat3697.
[59] A. Capelo, D. Fattoruso, L.C. Valencia-Valero, M.A. Esteves, C.M. Rangel, A. Puga, Evolution of atomically dispersed co-catalysts during solar or UV photocatalysis for efficient and sustained H_2 production, Int. J. Hydrogen Energy 103 (2025) 645–658, https://doi.org/10.1016/j.ijhydene.2025.01.203.
[60] A. Patsoura, D.I. Kondarides, X.E. Verykios, Photocatalytic degradation of organic pollutants with simultaneous production of hydrogen, Catal. Today 124 (2007) 94–102, https://doi.org/10.1016/j.cattod.2007.03.028.
[61] D.I. Kondarides, V.M. Daskalaki, A. Patsoura, X.E. Verykios, Hydrogen Production by Photo-Induced Reforming of Biomass Components and Derivatives at Ambient Conditions, Catal Lett 122 (2008) 26–32, https://doi.org/10.1007/s10562-007-9330-3.
[62] L. Lan, H. Daly, R. Sung, F. Tuna, N. Skillen, P.K.J. Robertson, C. Hardacre, X. Fan, Mechanistic Study of Glucose Photoreforming over TiO_2 -Based Catalysts for H_2 Production, ACS Catal. 13 (2023) 8574–8587, https://doi.org/10.1021/acscatal.3c00858.
[63] R. Leary, A. Westwood, Carbonaceous nanomaterials for the enhancement of TiO_2 photocatalysis, Carbon 49 (2011) 741–772, https://doi.org/10.1016/j.carbon.2010.10.010.
[64] N. Lakshminarasimhan, W. Kim, W. Choi, Effect of the agglomerated state on the photocatalytic hydrogen production with in situ agglomeration of colloidal TiO_2 nanoparticles, J. Phys. Chem. C 112 (2008) 20451–20457, https://doi.org/10.1021/jp808541v.
[65] R.I. Bickley, T. Gonzalez-Carreno, J.S. Lees, L. Palmisano, R.J.D. Tilley, A structural investigation of titanium dioxide photocatalysts, J. Solid State Chem. 92 (1991) 178–190, https://doi.org/10.1016/0022-4596(91)90255-G.
[66] M. Asadsangabifard, C. Onn, J.J.H. Tam, Operational parameters effects on photocatalytic reactors of wastewater pollutant: A review, Desalin. Water Treat. 120 (2018) 109–118, https://doi.org/10.5004/dwt.2018.22723.
[67] M. Zhou, Y. Li, S. Peng, G. Lu, S. Li, Effect of epimerization of d-glucose on photocatalytic hydrogen generation over Pt/TiO_2, Catal. Commun. 18 (2012) 21–25, https://doi.org/10.1016/j.catcom.2011.11.017.
[68] M.R. Karimi Estahbanati, N. Mahinpey, M. Feilizadeh, F. Attar, M.C. Iliuta, Kinetic study of the effects of pH on the photocatalytic hydrogen production from alcohols, Int. J. Hydrogen Energy 44 (2019) 32030–32041, https://doi.org/10.1016/j.ijhydene.2019.10.114.
[69] A. Kumar, P. Sharma, G. Sharma, P. Dhiman, G.T. Mola, M. Farghali, A. K. Rashwan, M. Nasr, A.I. Osman, T. Wang, Simultaneous hydrogen production and photocatalytic pollutant removal: a review, Environ Chem Lett 22 (2024) 2405–2424, https://doi.org/10.1007/s10311-024-01756-w.